Journal of Controlled Release 379 (2025) 440–451

Contents lists available at ScienceDirect

Journal of Controlled Release

journal homepage: www.elsevier.com/locate/jconrel

Design, evaluation, and *in vitro–in vivo* correlation of self-nanoemulsifying drug delivery systems to improve the oral absorption of exenatide

Ramakrishnan Venkatasubramanian [a], Passant M. Al-Maghrabi [a], Oscar Alavi [a], Tania Lind [b], Philip Jonas Sassene [c], Jacob J.K. Kirkensgaard [d,e], Pablo Mota-Santiago [f], Thomas Rades [a,*], Anette Müllertz [a,b]

[a] Department of Pharmacy, University of Copenhagen, Universitetsparken 2, Copenhagen 2100, Denmark
[b] Bioneer A/S, Kogle Allé 2, Hørsholm 2970, Denmark
[c] Novo Nordisk A/S, Novo Nordisk Park 1, Maaloev 2760, Denmark
[d] Department of Food Science, University of Copenhagen, Frederiksberg C 1958, Denmark
[e] Niels Bohr Institute, University of Copenhagen, Universitetsparken 5, Copenhagen 2100, Denmark
[f] MAX IV Laboratory, Lund University, P.O. Box 118, Lund 22100, Sweden

ARTICLE INFO

Keywords:
Self-nanoemulsifying drug delivery systems (SNEDDS)
Oral peptide drug delivery
Exenatide
Design of experiments
Oral bioavailability
In vitro- in vivo correlation

ABSTRACT

The ability to predict the absorption of exenatide (Ex), a GLP-1 analogue, after oral dosing to rats in self-nanoemulsifying drug delivery systems (SNEDDS), using *in vitro* methods, was assessed. Ex was complexed with soybean phosphatidylcholine (SPC) prior to loading into SNEDDS. A design of experiments (DoE) approach was employed to develop SNEDDS incorporating medium-chain triglycerides (MCT), medium-chain mono- and diglycerides (MGDG), Kolliphor® RH40, and monoacyl phosphatidylcholine. SNEDDS with higher proportions of MGDG and Kolliphor® RH40 demonstrated a 9-fold reduction in droplet size (230 to 26 nm), a 1.5-fold decrease in lipolysis (0.23 to 0.34 mmol of FFA), and a 2-fold enhancement in exenatide protection against proteolysis (73 % to 38 %) compared to those with higher MCT content. Permeability studies in Caco-2 cells showed that SNEDDS with higher proportion of MGDG displayed a 40-fold increase in apparent permeability of FD4, when compared to SNEDDS with higher proportion of MCT. An oral gavage study in rats revealed a 1.8-fold higher absorption of Ex in SNEDDS with a higher proportion of MGDG and Kolliphor®RH40 compared to SNEDDS with higher MCT. These results establish a clear *in vitro–in vivo* correlation, demonstrating that the selected *in vitro* methods effectively differentiated formulations with high and low absorption of exenatide after oral dosing in rats.

1. Introduction

Upon oral administration, peptides are labile to acid and enzymatic hydrolysis and show poor permeability across the intestinal epithelium due to their large size and hydrophilicity. Self-nanoemulsifying drug delivery systems (SNEDDS) potentially improve absorption of peptides [1] as they may provide proteolytic protection and have innate permeation enhancing abilities [2–6] to facilitate either paracellular or transcellular transport [7–9]. However, the hydrophilicity of therapeutic peptides makes it challenging to load them into the lipophilic SNEDDS preconcentrate (*i.e.* a SNEDDS formulation before dispersion).

One approach to improve the lipophilicity of peptides is *via* complexation with phospholipids, such as soybean phosphatidylcholine (SPC). Insulin has previously been complexed with SPC using freeze-drying prior to loading into SNEDDS preconcentrates. Complexation of insulin with SPC improved its lipophilicity [10], and loading the complex into SNEDDS protected insulin against proteolytic enzymes, enabled a better transport across cell monolayers, and improved intestinal absorption compared to an aqueous insulin solution [10,11].

Despite the considerable potential of SNEDDS in overcoming the challenges associated with oral peptide delivery, the design and optimization of these systems remain empirically driven. While prior

* Corresponding author.
E-mail addresses: venkatasubramanian.ramakrishnan@sund.ku.dk (R. Venkatasubramanian), passant.almaghrabi@sund.ku.dk (P.M. Al-Maghrabi), oscar@alavi.dk (O. Alavi), tkl@bioneer.dk (T. Lind), pjsa@novonordisk.com (P.J. Sassene), jjkk@food.ku.dk (J.J.K. Kirkensgaard), pablom@ansto.gov.au (P. Mota-Santiago), thomas.rades@sund.ku.dk (T. Rades), anette.mullertz@sund.ku.dk (A. Müllertz).

https://doi.org/10.1016/j.jconrel.2025.01.013
Received 28 April 2024; Received in revised form 4 December 2024; Accepted 6 January 2025
Available online 16 January 2025

research has demonstrated the capacity of SNEDDS to enhance peptide bioavailability through various mechanisms such as permeability [2,7], and proteolytic protection [12–14], the underlying properties that govern these effects have not been systematically elucidated. This represents a significant gap in the development of rational, peptide-specific SNEDDS formulations.

In the present study, an optimized exenatide (Ex) (a 39-amino acid GLP-1 analogue, with a molecular weight of 4.2 kDa) complex with SPC (Ex:SPC complex) was prepared and added to various SNEDDS preconcentrates. For the SNEDDS preconcentrates medium chain (C_8-C_{10}) triglycerides (MCT), medium chain (C_8-C_{10}) mono-diglycerides (MGDG), and monoacyl-phosphatidylcholine (MAPC), were selected as excipients for a design of experiments (DoE) based formulation approach [4,11,14]. Protection of Ex from proteolysis was evaluated by an *in vitro* proteolysis assay. The initial droplet size and rate and extent of digestion were investigated by dynamic light scattering, *in vitro* lipolysis and small -angle X-Ray scattering (SAXS). The ability of the DoE designed SNEDDS to open tight junctions was evaluated in Caco 2 cell monolayers.

The objective of this study was to assess the ability of the above mentioned *in vitro* methods applied on the DoE designed Ex:SPC complex containing SNEDDS to predict the absorption of Ex after oral gavage in rats.

2. Materials

Ex was gifted from Bachem (Basel, Switzerland). SPC (Lipoid S 100 (phosphatidylcholine from soybean; not less than 94.0 % pure) and MAPC (Lipoid P LPC 80 (lyso-phosphatidylcholine (LPC) from soybean, containing 80.0 % LPC) were donated by Lipoid (Ludwigshafen, Germany). Medium chain (C_8-C_{10}) triglycerides (MCT; Captex 300 EP/NF) and C_8-C_{10} mono-diglycerides (Capmul MCM EP/NF; MGDG)) were gifted from Abitec (Janesville, WI, USA). Polyoxyl 40 hydrogenated castor oil (Kolliphor® RH 40) was donated by BASF (Ludwigshafen, Germany). Calcium chloride anhydrous was purchased from Merck KGaA (Darmstadt, Germany). α-Chymotrypsin (α–CT) from bovine pancreas (type II, lyophilized powder, ≥40 units/mg protein), bovine bile, fluorescein isothiocynate dextran-4 (4 kDa; FD4), 4-(2-hydroxyethyl)-1-piperazineethanesulfonic acid (HEPES), t-octylphenoxypolyethoxyethanol (Triton™ X-100) and porcine pancreatin extract were obtained from Sigma-Aldrich (St Louis, MO, USA). Lithium heparin coated plasma tubes were purchased from Sarstedt (Nümbrecht, Germany). Deionized water was obtained from an SG Ultraclear water system (SG Water GmbH, Barsbüttel, Germany). All other reagents used were of analytical grade. The compositions of lipid excipients is described in Table S1.

3. Methods

3.1. Preparation and characterization of ex:SPC complexes

Ex:SPC complexes were prepared by freeze-drying (Lyoquest, Telstar, Terrassa, Spain) as described in Fong *et. al* with minor modifications [15]. Briefly, different molar (and weight) ratios of Ex (2 mg) to SPC (1:2 (1:0.4), 1:4 (1:0.8), 1:6 (1:1.1), 1:12 (1:2.2), 1:18 (1:3.4), 1:30 (1:5.6), 1:60 (1:11.2) and 1:120 (1:22.4)) were dissolved in a solution 0.4 mL of tertiary butyl alcohol and water (containing 5 % *v/v* acetic acid) at a ratio of 60:40 *w/w* and stirred at 37 °C (approximately 20 min). The prepared solutions were frozen for 2 h at -80 °C. The freeze-drying program included a primary drying phase at -20 °C at 0.05 mBar for 16 h; followed by a secondary drying phase at 25 °C at 0.1 mBar for 2.5 h. To account for any residual solvents, the vials with Ex and SPC were weighed before addition of solvents and once again after the completion of the freeze-drying process. A weight difference (before and after freeze drying) of less than 1 % was considered acceptable.

The vials were then screw-capped, sealed with parafilm and stored at -80 °C until use.

The lipophilicity of the generated Ex:SPC complexes was evaluated by determining the miscibility and retention of Ex in MGDG.

For the miscibility studies, the prepared ratios of Ex:SPC (2 mg Ex) were stirred on a magnetic stirrer in 1 mL MGDG for 24 h at room temperature (RT), followed by centrifugation (10 min at 17,004*g* at 25 °C). The resulting clear supernatant and pellet were quantified for Ex using RP-HPLC-UV (described below).

For the partition studies, the prepared Ex:SPC complexes (2 mg Ex) were added to 2 mL of MGDG:PBS (pH 6.8) (1:1 (*v/v*)), and stirred on a magnetic stirrer for 24 h at RT. The samples were centrifuged (10 min at 17,004*g* at 25 °C) to obtain two phases (MGDG and PBS), which were both analyzed for the presence of Ex. As controls, Ex alone and physical mixtures of Ex and SPC (Ex+SPC) were used in the miscibility and partition studies. Additional interactions were characterized using SAXS, as described in Section S1.

3.2. Development and characterization of SNEDDS

3.2.1. Design of experiments to develop SNEDDS preconcentrates

For the DoE, lipid excipients were used in the following ranges; MCT: 30–60 % *w/w*, MGDG: 10–45 % *w/w*, and Kolliphor®RH40: 10–30 % *w/w*. MAPC was kept constant at 10 % w/w. A DoE generated by MODDE 13 software (Umetrics, Sweden) with D-optimal design, was used to determine the composition of the SNEDDS preconcentrates. This gave 15 SNEDDS preconcentrates, including three center points as displayed in Table 1. The SNEDDS preconcentrates were prepared by weighing the excipients into screw-capped glass vials and mixing in an IntelliMixer (ELMI, Riga, Latvia) at 250 rpm at 37 °C until homogenous.

3.2.2. Droplet size measurements

The SNEDDS preconcentrates were dispersed in 10 mM HEPES buffer (pH 6.8) at a ratio of 1:100 *v/v* followed by gentle end-over-end rotation by hand for one minute. The droplet size was measured using dynamic light scattering (DLS) in a Zetasizer Nano ZS (Malvern Panalytical, Malvern, UK) and are reported as *Z*-average. The scattering angle was set at 173° and the refractive index at 1.33 with a viscosity of 0.69 cP at 37 °C.

Additionally, stability of the selected SNEDDS were performed at 37 °C for 4 h (Data presented in Fig. S6).

3.2.3. In vitro lipolysis

The *in vitro* lipolysis set-up consisted of a pH-stat instrument, with an 804 Ti Stand, a Titrando 842, an 802 stirrer, a glass pH electrode and two Dosino dosing units coupled to two 10 mL autoburettes (Metrohm AG, Herisau, Switzerland). The set up was operated by the Tiamo 2.5

Table 1
Composition of SNEDDS preconcentrates based on the D-optimal design. MAPC was kept constant at 10 % w/w.

	Lipid Excipients (*w*/w %)		
Formulations	MCT	MGDG	Kolliphor® RH40
N1	60	10	20
N2	30	45	15
N3	60	20	10
N4	35	45	10
N5	35	45	10
N6	50	10	30
N7	30	30	30
N8	30	35	25
N9	60	17	13
N10	53	10	27
N11	52	28	10
N12	37	23	30
N13	44	27	19
N14	44	27	19
N15	44	27	19

software (Metrohm AG, Herisau, Switzerland). The SNEDDS pre-concentrates (1.0 g) from the DoE were initially pre-dispersed in 20 mL simulated intestinal fluid (SIF; Table S2) in a thermostatic vessel (37 °C). The pH of the dispersion was manually adjusted to 6.5. A pancreatic enzyme solution was prepared by weighing out the required amount of porcine pancreatin extract and vortexing it with 6.0 mL of SIF, followed by centrifugation (7 min, 4500 *g* at 4 °C). To initiate the lipolysis, 5.0 mL of fresh pancreatic enzyme solution (pH 6.5) was added to the dispersion to obtain a lipase activity of 179 USP/mL. The pH was maintained at 6.5 for 60 min by adding 0.4 M NaOH from the auto-burette. Calcium was added (as 0.5 M $CaCl_2$) continuously (0.01 mL/min) to control the rate of lipolysis [16].

3.2.4. *In vitro proteolysis*

Ex (2 mg; as Ex:SPC) was loaded in the designed SNEDDS pre-concentrates (1 g) by gently stirring at 37 °C for at least 6 h. The Ex:SPC-SNEDDS were dispersed in 5 mL of 10 mM HEPES (37 °C, pH 6.5) under magnetic stirring. Proteolysis was initiated by adding α-CT (0.25 U/mL). Samples (200 μL) were withdrawn at time points 0 (before adding α-CT), 5, 15, 30, 45 and 60 min. To inhibit the proteolysis, 200 μL of ice-cold 0.1 % Triton X-100 (to dissolve the SNEDDS) with 1 % trifluoroacetic acid (TFA; to inhibit the activity of α-CT) was added to each sample. Samples were then centrifuged (10 min, 9600 *g* at 4 °C) and the clear supernatant was diluted appropriately in acetonitrile prior to injection into the RP-HPLC. Intact Ex at each time point was quantified by RP-HPLC (see Section 3.6). The amount of Ex protected was calculated as the amount of intact Ex at each time point, normalized by the Ex concentration at 0 min. The amount of Ex protected at 60 min of proteolysis was entered into the MODDE 13.0 software for data modelling. Ex alone, Ex+SPC, Ex:SPC complex and SNEDDS loaded with Ex alone were utilized as controls for the *in vitro* proteolysis study.

3.3. *In vitro lipolysis studies by in situ SAXS of selected SNEDDS*

In situ SAXS measurements were performed at MAX-IV laboratory (Lund, Sweden) at the CoSAXS beamline with a photon energy of 12.4 keV and a sample-to-detector distance of 886 mm. The sample-to-detector distance was calibrated using silver behenate. The *in vitro* lipolysis was carried out as described in section 4.2.3. A peristaltic pump was used to pump the lipolysis medium in a loop from the digestion vessel through a quartz capillary (1.5 mm in diameter) mounted in the X-ray beam for studying the time evolution of digestion peaks in real-time SAXS monitoring (acquisition time of 2 s per measurement) during the *in vitro* lipolysis experiments and then returned to the digestion vessel [17]. The same lipolysis method as described in *4.2.3* was used for these lipolysis experiment. SNEDDS preconcentrate (1 g) was dispersed in the SIF and the titration program was started after an initial 5 min delay. During the 5 min delay, the pH was monitored and correlated to SAXS measurements carried out with an acquisition time of 2 s per frame and a delay of 8 s for 60 s total, as well. After collecting the initial scattering curves of the SNEDDS dispersion, digestion was initiated by injection of freshly prepared pancreatic lipase extract using a remotely activated syringe driver. At this point the titration program was started and the pH of the SNEDDS dispersion was maintained at 6.5 by adding 1 M NaOH. Calcium was added (as 0.5 M $CaCl_2$ at 0.01 mL/min) continuously during the digestion. SAXS data was acquired every 20 s with an acquisition time of 2 s per frame and a delay of 18 s for one hour. The 2D SAXS patterns were collected by an Eiger 2 X 4 M detector (Dectris, Baden-Dättwil, Switzerland) and average in the azimuthal direction. All the SAXS data were normalized and subsequently background corrected by subtracting the SAXS scattering intensity of the empty capillary and the digestion of buffer using OriginPro 2020 software version 9.7.0.188 (OriginLab Corp., Northampton, MA, USA). The d-spacing, or the lattice parameter, of the lamellar phase was calculated using the equation $d = 2\pi/q$ where q is the location of the first lamellar phase peak. The obtained area under the curves (AUCs) were normalized with the AUC of each of the SNEDDS at time zero. The detected lamellar phase peaks were fitted to Lorentz functions using the OriginPro 2020 software to estimate the normalized area under the curve of the observed Bragg peaks.

3.4. *In vitro permeability studies in Caco-2 cells*

The human colorectal adenocarcinoma cell line Caco-2 provided by the American Type Culture Collection (Manassas, VA, USA) was used for the permeability studies. Caco-2 cells were grown in Dulbecco's Modified Eagle's Medium supplemented with fetal bovine serum (10 % *v/v*), penicillin (100 U/mL), streptomycin (100 μg/mL) and non-essential amino acids (1 % *v/v*) in a humidified 5 % CO_2 incubator at 37 °C with replacing the culture medium every two days for 21 days. The cells were seeded in 12-Transwell® plates on polycarbonate membrane inserts (1.13 cm^2, pore size of 0.4 μm; Corning, NY, USA) at a final density of 2×10^5 cells/cm^2.

The transport studies were performed using 25 mM MES (pH 6.5, 0.05 % *w/v* BSA) and 25 mM HEPES (pH 7.4, 0.05 % w/v BSA) as the donor and acceptor medium, respectively, with horizontal shaking (75 rpm) at 37 °C. The SNEDDS were dispersed (1:100 *v/v*) in MES buffer, pH 6.5, with FD4 at a final concentration of 1 mg/mL. To initiate the transport study, 500 μL of the dispersion was added to the donor chamber, using 1 mg/mL FD4 in MES as a control. During the experiments, 200 μL samples were withdrawn from the acceptor chamber at 15, 30, 45, 60, 90 and 120 min and replaced with 200 μL preheated (37 °C) HEPES buffer. The integrity of the cell monolayers was monitored using trans-epithelial electrical resistance (TEER) on an EVOM™ Meter coupled with Endohm™ chamber (World Precision Instruments, Sarasota, FL, USA) in MES buffer (0 min) and after the addition of SNEDDS dispersions (120 min) during the permeability study.

The cumulative permeated amount of FD4 was determined using a microplate reader (CLARIOStar® plus, Germany) at 492 ± 8 nm excitation and 520 ± 8 nm emission wavelengths. The apparent permeability coefficient (P_{app}, cm/s) was calculated according to Eq. (1):

$$Papp = \frac{dQ}{dt}_{*}\frac{1}{A*Co} \quad (1)$$

where dQ/dt is the steady state flux (μg/s), A is the surface area of the Transwell® membrane inserts (1.13 cm^2), and Co is the initial FD4 concentration in the donor compartment (μg/mL). All experiments were performed in triplicates across three passages of Caco-2 cells.

3.5. *Pharmacokinetic studies in rats*

The animal study was conducted under license no. 2019-15-0201-00262 and was approved by the Animal Welfare Committee, appointed by the Danish Ministry of Justice. All procedures on animals were carried out in compliance with EC Directive 86/609/EEC and with the Danish laws regulating experiments on animals. Male Sprague-Dawley rats (Janvier lab, Saint Berthevin, France) with an average weight of 270 ± 13 g were kept in the animal care facility under an inverted light cycle, standard food and water *ad libitum* for one week before entering the study. To reduce stress on the day of the experiments, the rats were handled every day during this week by the operator. Prior to the day of the experiments, the rats were fasted for at least 12 h with water available *ad libitum*.

The animals were divided into five groups of six rats, and randomly assigned to receive one of five formulations. The positive control group received a subcutaneous (*s.c.*) solution of Ex (dissolved in sterile isotonic saline; 30 μg). The negative control group received Ex solution (150 μg/mL; dissolved in sterile water). The remaining three groups were administered 150 μg Ex (as Ex:SPC complex) in the three selected SNEDDS preconcentrates (80 μL; N1, N4, and N7 SNEDDS) by oral gavage. The relative bioavailability of orally administered Ex was

calculated using Eq. (2):

$$\textit{Relative Bioavailability}\ (\%) = \frac{[(AUCoral)*(Dosesc)]}{[(AUCsc)*(Doseoral)]} \quad (2)$$

where the AUC is the area under the curve of the Ex plasma concentration *vs* time profile for exenatide dosed orally or *via s.c.* injection.

Blood samples of 200 μL were collected by tail vein puncture into heparin coated tubes containing enzyme inhibitor (25 μL added to each tube which contains 250 KIU aprotinin). Blood samples were taken at time 0 (before dosing), and 0.5, 1.0, 1.5, 2.0, 2.5, 3.0, 4.0, 6.0, and 8.0 h after dosing. The animals were killed (in a CO_2 gassing chamber) immediately prior to the last blood sample at 8.0 h, which was collected from the heart. To prevent degradation of Ex in harvested blood samples, plasma was separated immediately by centrifugation (10 min at 6708 *g* at 4 °C) and stored at -80 °C until quantification of Ex using ELISA (FEK-070-94; Phoenix Pharmaceuticals, USA).

3.6. RP-HPLC analysis of exenatide

A Dionex Ultimate 3000 system (Thermo Fischer Scientific, Waltham, MA, USA) was used to analyze Ex containing samples with an injection volume of 25 μL and a column temperature of 25 °C. Ex was quantified utilizing the AUC of the UV absorbance peak at 276 nm, with a new standard curve for each study, ranging from 5 to 250 μg/mL.

3.6.1. Quantification of Ex from the miscibility and partition studies in MGDG

Separation of Ex was carried out on a Kinetex C18 column (100 x 4.6 mm, 5 μm; Phenomenex Torrance, CA, USA). The mobile phases used were, A: 0.1 % *v/v* TFA in deionized water and B: 0.1 % *v/v* TFA in acetonitrile. The following gradient was applied with a flow rate of 0.8 mL/min and an injection speed of 10 μL/s: 0–2 min A:B (80:20, *v/v*), 2–12 min A:B (80:20 to 20:80, *v/v*), 12–15 min A:B (20:80, *v/v*), 15–17 min A:B (20:80 to 80:20, *v/v*) and 17–18 min (80:20, *v/v*). Limit of Detection: 2.8 μg/mL; Limit of Quantification: 8.9 μg/mL.

3.6.2. Quantification of Ex from the proteolysis study

Separation of Ex was carried out on a Luna 5u C18 (2) column (250 x 4.6 mm, 5 μm; Phenomenex Torrance, CA, USA). The same mobile phases as above were utilized. The flow rate was set at 1.0 mL/min, and the injection speed was 1 μL/s. The gradient used was as follows: 0–1 min A:B (85:15 to 63:37, *v/v*), 1–4.5 min A:B (63:37 to 56:44, *v/v*), 4.5 to 5 min A:B (56:44 to 5:95, *v/v*), 5–5.5 min A:B (5:95, *v/v*), 5.5–6 min (5:95 to 85:15, *v/v*), and 6–9 min (85:15 *v/v*). Limit of Detection: 5.3 μg/mL; Limit of Quantification: 16 μg/mL.

3.7. Data analysis

Data analysis was performed using either Microsoft Excel 2016 (Microsoft Office, Redmond, WA, USA) or GraphPad Prism 9 (GraphPad Software, San Diego, CA, USA). All statistical analyses were performed using GraphPad Prism 9. Statistical differences between the groups were analyzed using one-way ANOVA ($p = 0.05$) followed by Tukey's *post hoc* test. Correlations between the applied *in vitro* methods were determined using Pearson correlation coefficient.

4. Results and discussion

4.1. Characterization of the Ex:SPC complexes

4.1.1. Lipophilicity of the Ex:SPC complex

Fig. 1a and b show the miscibility and retention of 2.0 mg of Ex as a complex with SPC at different molar ratios. Upon increasing the molar ratio between Ex and SPC from 1:2 to 1:120, the miscibility in MGDG increases (from 69 ± 12 to 1854 ± 179 μg/mL). Likewise, partitioning of Ex into the MGDG phase (as Ex:SPC) increases upon increasing the molar ratio between Ex and SPC (from 108 ± 12 (at 1:2) to 1932 ± 4 μg/mL (at 1:120)). Miscibility and partition studies of the controls (Ex alone and Ex+SPC), revealed that Ex was not miscible in MGDG (< 10 μg/mL) and that almost all the Ex (> 1900 μg) partitioned into the PBS phase. This indicates the necessity of complexation to improve miscibility and retention of Ex in MGDG. Comparable results were obtained by Zhou et al. who showed that insulin needed to be complexed with SPC in order to improve its miscibility in MCT [18].

Ex has both positively (4 sites) and negatively (6 sites) charged amino acids, suggesting potential interactions with anionic or cationic counter ions [19]. However, at lower molar ratios of Ex:SPC (such as 1:4 or 1:6), less Ex was miscible and retained in MGDG, and a maximum miscibility and retention was observed at molar ratios of 1:60 and 1:120. The increased miscibility and retention of Ex in MGDG is thus most likely due to lipid-enabled miscibility or retention in MGDG, and not due to charge based interactions. The interactions between Ex and SPC were evaluated by using SAXS on the 1:60 complex. This is displayed in *Section S1.2.* of the supplementary information. The diffractograms suggests a change in packing of SPC upon freeze drying with Ex as Ex:

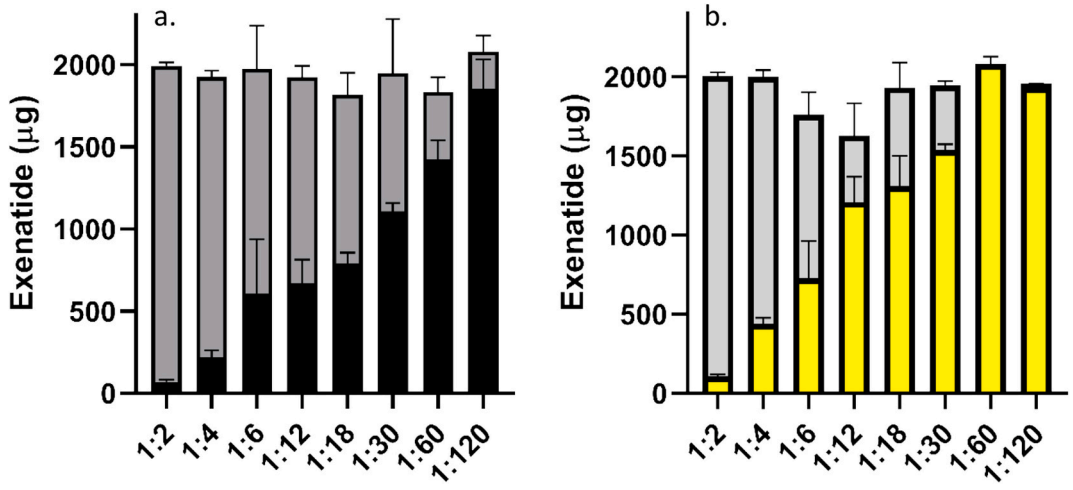

Fig. 1. a. Miscibility of 2.0 mg of Ex (at different molar ratios of Ex:SPC) in C_8-C_{10} mono-diglycerides (MGDG) at room temperature (RT). The black bars represent Ex in MGDG supernatant, whereas the grey bars represent Ex in the pellet after centrifugation; **b.** Partition of 2.0 mg of Ex (as Ex:SPC) between MGDG and phosphate buffered saline (PBS, pH 6.8 at RT). The yellow bars represent Ex in the MGDG phase, whereas the light grey bars represent Ex in the PBS phase. All data are expressed as mean ± SD; $n = 3$. (For interpretation of the references to colour in this figure legend, the reader is referred to the web version of this article.)

SPC (disappearance of inverse micellar phase (L_2 phase)), compared to SPC alone or Ex+SPC. No statistical difference in miscibility ($p = 0.0501$) or partition ($p = 0.7983$) of Ex was found at molar ratios 1:60 and 1:120 of Ex:SPC. Thus, Ex:SPC at 1:60 was chosen for further studies.

4.2. Development and evaluation of the DoE generated SNEDDS

4.2.1. Droplet size analysis of SNEDDS dispersion

The droplet size distribution of the emulsions generated by dispersion of the DoE generated SNEDDS (Table 1) ranged from 20 to 230 nm. Individual droplet sizes (*Z*-average) and polydispersity indices (PdI) for the SNEDDS dispersions are shown in Table S3. The model for the resulting droplet sizes of the SNEDDS generated by MODDE, is presented in Fig. 2a, b and c as a response contour plot, observed *vs* predicted droplet size (nm), and equation coefficients for droplet size (nm), respectively. The model fit (R [2]) and prediction power (Q [2]) were 0.97 and 0.91, respectively (Fig. 3b), indicating a valid model [20]. As expected, Kolliphor®RH40 and MGDG reduce the droplet size, whereas MCT increases it (Fig. 2c). This can be seen in the contour plot (Fig. 2a), where SNEDDS consisting of a higher fraction of MCT (*e.g.* N1; 60/10/20 % MCT/MGDG/Kolliphor®RH40) had a larger size (231 nm). Upon increasing the fraction of MGDG (*e.g.* N4; 35/45/10 % MCT/MGDG/Kolliphor®RH40), the droplet size reduced to 88 nm. Further, upon increasing the fraction of the hydrophilic surfactant Kolliphor®RH40 (*e.g.* N7; 30/30/30 % MCT/MGDG/Kolliphor®RH40) the droplet size reduced to 23 nm.

4.2.2. In vitro lipolysis of SNEDDS dispersion

The amount of free fatty acid (FFA; mmol) generated after 60 min of *in vitro* lipolysis was analyzed by MODDE and revealed an R^2 and a Q^2 of 0.91 and 0.87 respectively, indicating a valid model. Fig. 3a, b and c display the response contour plot, observed *vs* predicted lipolysis (FFA; mmol), and equation coefficients for the *in vitro* lipolysis, respectively. The profile of FFA generation during *in vitro* lipolysis is shown in Fig. S2. Based on Fig. 3c, MCT plays a significant role in increasing the lipid digestion (as seen in N1; 0.36 mM), whereas the Kolliphor®RH40 content significantly reduces lipolysis (N4 (0.29 mM) and N7 (0.25 mM)). The MGDG content did not play a significant role for lipolysis within the design space (Fig. 3c), which is surprising as diglycerides are a substrate for pancreatic lipase, and the used MGDG contains 35 % diglycerides (Table S1). However, this might still be too low a level to influence lipolysis. The amount of MCT in SNEDDS increases the release of FFA during lipolysis, as MCT is a substrate for pancreatic lipase. On the other hand, Kolliphor®RH40 is not a substrate for pancreatic lipase and therefore did not play a role for the extent of lipolysis [21].

4.2.3. In vitro proteolysis of Ex in Ex:SPC-SNEDDS

Fig. 4a, b and c represent the response contour plot of %Ex protected from proteolysis after 60 min, observed *vs* predicted protection of Ex, and equation coefficients for Ex protection, respectively. The ability of the Ex:SPC-SNEDDS to protect Ex from proteolysis over time is shown in Fig. S3. After 60 min of proteolysis, the percentage of Ex that was not hydrolyzed (% exenatide protected) ranged from 40 to 78 % (Fig. 4a). The amount of Ex protected by Ex:SPC-SNEDDS after 60 min of

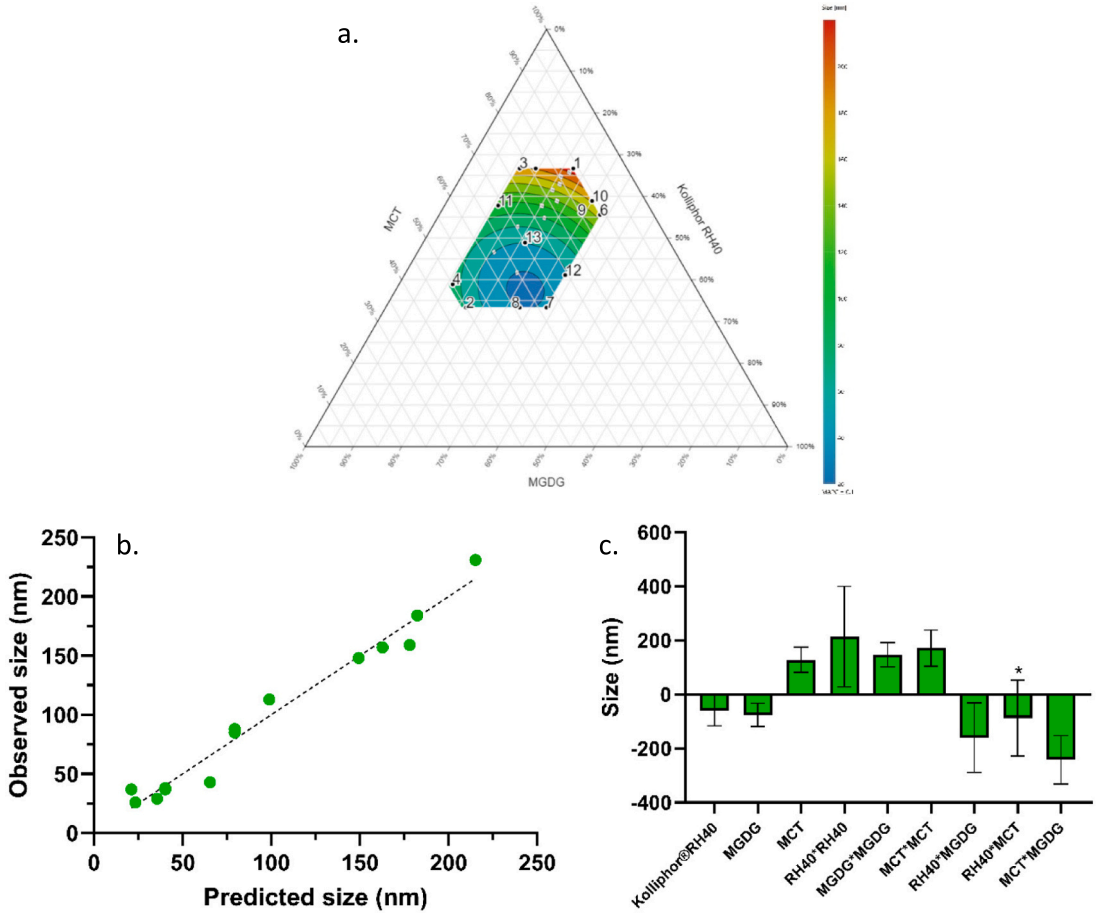

Fig. 2. a. Response contour plot of the model generated for droplet size (nm) measured using dynamic light scattering (DLS) of the 15 SNEDDS listed in Table 1, dispersed in 10 mM HEPES (pH 6.8); **b.** Observed *versus* predicted droplet size (nm) of SNEDDS dispersion; **c.** Coefficients corresponding to the linear and quadratic equation terms for droplet size (nm) as a response. The asterisk (*) signifies a coefficient term which has an insignificant effect on the response (droplet size of SNEDDS) value.

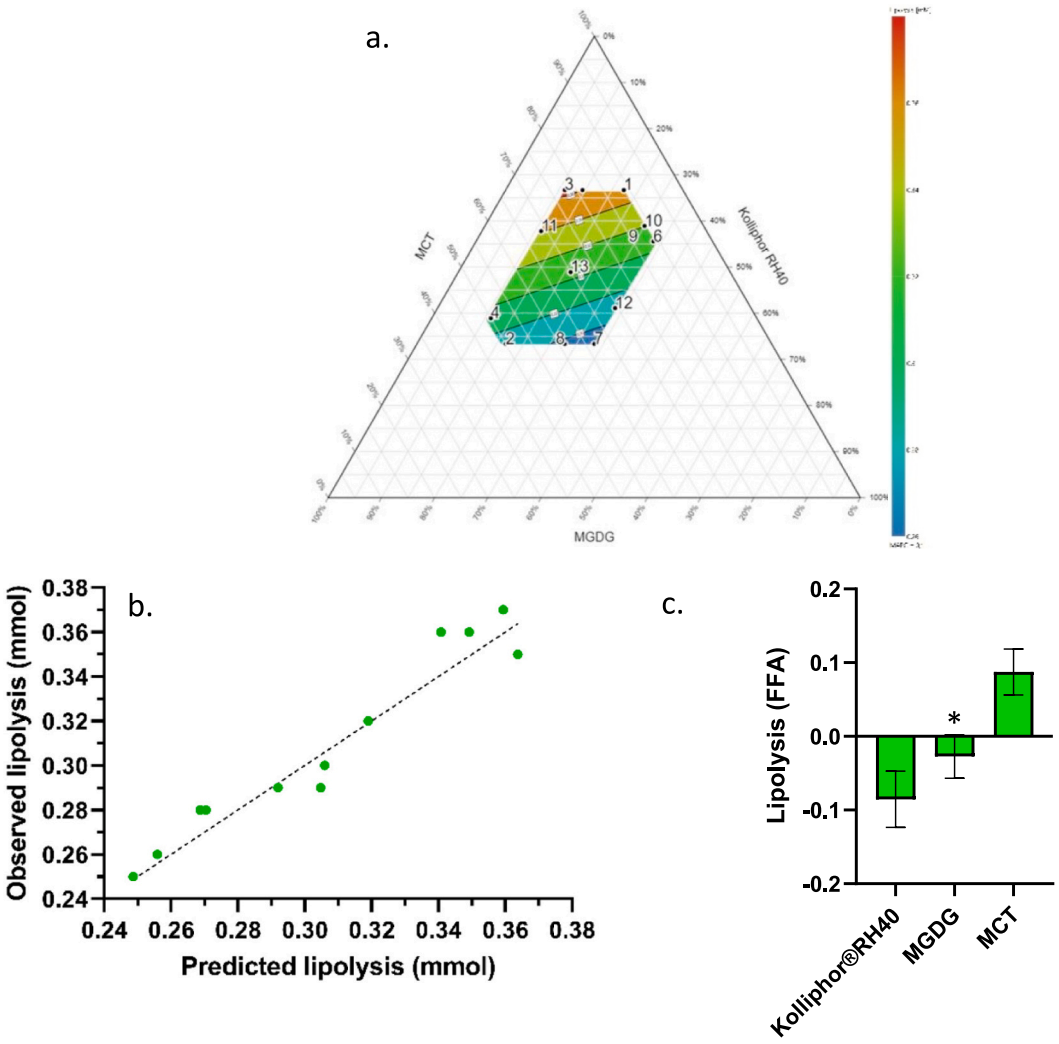

Fig. 3. a. Response contour plot of the model generated for depicting free fatty acid (FFA; mmol) released after 60 min of *in vitro* lipolysis of SNEDDS containing C_8-C_{10} triglycerides (30–60 % *w*/w; MCT), C_8-C_{10} monoglycerides (10–45 % w/w; MGDG), Kolliphor® RH40 (10–30 % *w*/w) and monoacyl phosphatidylcholine (MAPC; 10 % w/w); **b.** Observed *versus* predicted lipolysis of SNEDDS dispersion in the *in vitro* dynamic lipolysis model; **c.** Coefficients corresponding to the linear equation terms for lipolysis (FFA; mmol) as a response. The asterisk (*) signifies a coefficient term which has an insignificant effect on the response (lipolysis of SNEDDS) value.

proteolysis displayed an R^2 and a Q^2 of 0.91 and 0.82 respectively, indicating a valid model. MGDG has a significant role in reducing the proteolytic degradation of Ex (*e.g.* N7; 78 % protection; 30 % MGDG), whereas higher MCT leads to reduced Ex protection (*e.g.* N1 SNEDDS with 10 % MGDG providing only 40 % protection), while increasing Kolliphor® RH40 significantly decreases the amount of Ex that is protected. This maybe due to the increased hydrophobicity of SNEDDS with higher fractions of MCT, leading to lower affinity of the Ex:SPC complex to reside within the colloidal structures formed, compared to SNEDDS with higher fractions of Kolliphor® RH40. Furthermore, according to the model, higher fractions of MGDG (*e.g.* N4 SNEDDS; 64 % protection; 45 % MGDG) may possibly reduce protection of Ex, as observed from the squared term (MGDG*MGDG) of the model. Ex alone, Ex+SPC, Ex:SPC complex and SNEDDS loaded with Ex alone did not offer any protection of Ex during 60 min of proteolysis. Comparable results were obtained by Liu et al. where complexation of insulin with SPC and loading in SNEDDS resulted in higher protection against α-CT, compared to insulin alone in SNEDDS, indicating that complexation is necessary for SNEDDS to be able to protect peptides from proteolysis [14].

4.2.4. Correlations between the different in vitro properties of the SNEDDS

Fig. 5 a, b and c represents the correlation plots between lipolysis *vs* size, lipolysis *vs* protection and size *vs* protection respectively, along with the Pearson correlation coefficient (*r*) within this design space.

As shown in Fig. 5a, the extent of lipolysis significantly increases when the droplet size increases ($p < 0.0001$; $r = 0.8474$). Larger droplets possess a lower total interfacial area compared to smaller droplets and could therefore be expected to display a lower extent of lipolysis. However, SNEDDS with larger droplets also contain higher fractions of MCT (*e.g.* N1), which is a good substrate for pancreatic lipase, relative to the other SNEDDS excipients utilized in this study (MGDG and Kolliphor®RH40), leading to higher lipolysis extent for larger droplets. The extent of lipolysis and protection of Ex from proteolysis displays a moderate inverse relationship, indicating that SNEDDS with a higher extend of lipolysis, also tend to be less efficient in protecting Ex ($p = 0.0085$; $r = -0.6516$). This suggests that excipients which are susceptible to lipase catalyzed lipid digestion (MCT and MGDG; present in higher fractions in N1 and N4 SNEDDS) tend to be less favorable in protecting Ex from proteolysis, and *vice versa* (*e.g.* N7 SNEDDS; relatively lower fraction of MCT and MGDG). The obtained results are in agreement with studies by Leonaviciute et al. and Mahjub et al., who reported that protection of lipid droplets from lipid digestion increases the proteolytic stability of peptide [22,23]. As a consequence of the observations shown in Fig. 5a and b, a larger droplet size

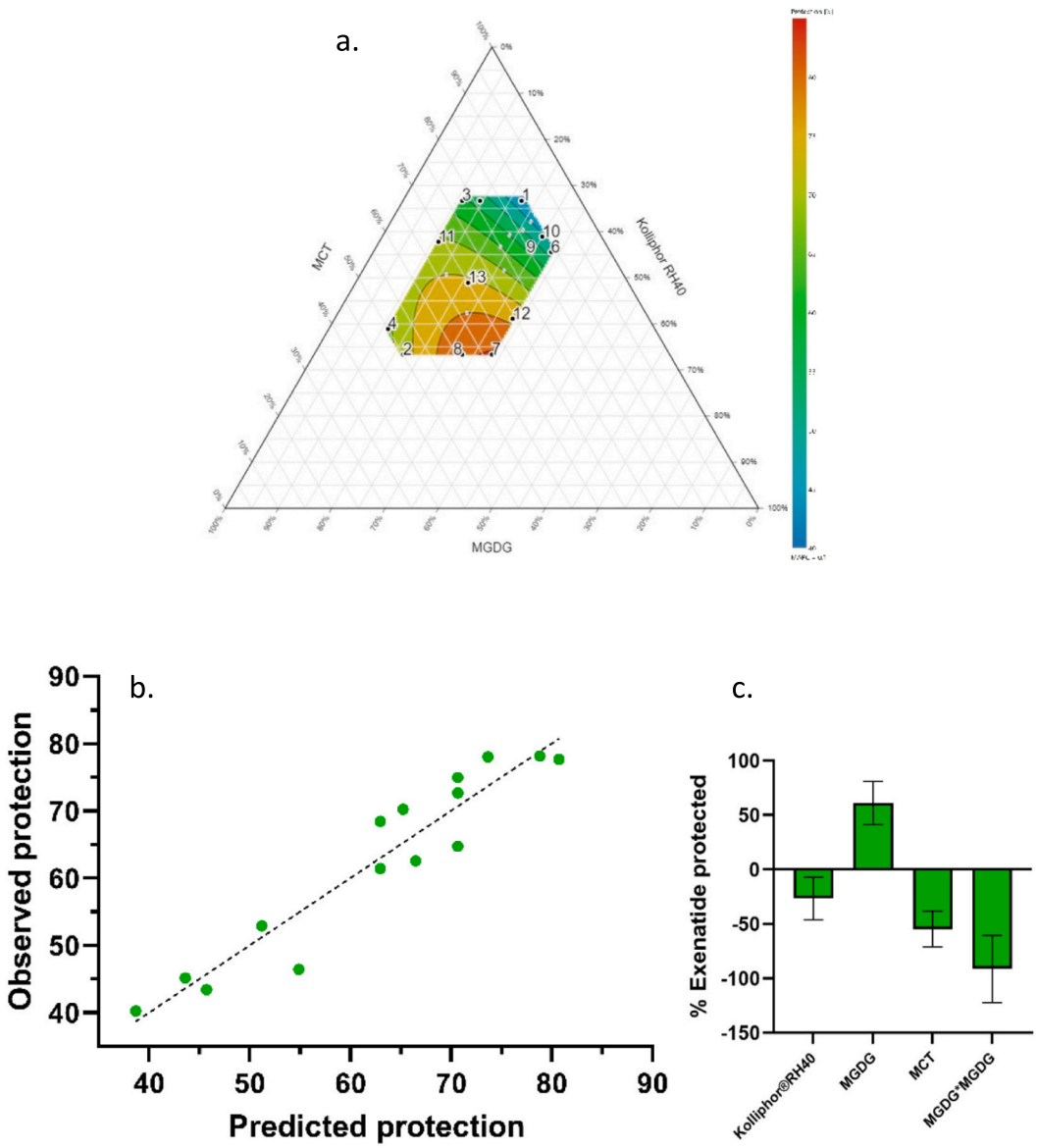

Fig. 4. **a.** Response contour plot of the model generated for %Ex protected after 60 min of *in vitro* proteolysis (using 0.25 U/mL of α-chymotrypsin) for Ex (as Ex:SPC) loaded SNEDDS preconcentrates containing MCT, MGDG, Kolliphor® RH40 and MAPC.; **b.** Observed *versus* predicted proteolysis of Ex:SPC-SNEDDS in the *in vitro* proteolysis model; **c.** Coefficients corresponding to linear and quadratic equation terms.

significantly reduces the proteolytic protection of Ex ($p < 0.0001$; $r = -0.8884$). This is in contrast to findings of Liu et al. and Hetényi et al., who observed increased proteolytic protection of peptides in SNEDDS with larger droplet size [14,24] albeit utilizing a larger size range (20 to 1250 nm), compared to this study (20 to 230 nm).

In summary, within the given design space, SNEDDS with smaller droplet size and lower lipid digestion tend to give better protection of Ex against α-CT. To assess the impact of these properties on the colloidal structures formed during lipolysis (*in situ* SAXS), *in vitro* permeability and *in vivo* absorption of Ex, three SNEDDS with different properties (Table 2) were selected.

4.3. *In situ SAXS during lipolysis of the selected SNEDDS*

The SAXS intensity *vs* scattering vector profiles during the lipolysis of the N1, N4 and N7 SNEDDS are presented in Fig. 6 a, b, and c, respectively. Before addition of pancreatin ($t = 0$ min), N1, N4 and N7 display a "bump" in the q-range of 0.05–0.15 $Å^{-1}$ (Fig. S4). This may be due to the presence of smaller colloidal structures that are generated during the dispersion [25,26]. The bump is more prominent in N7 possibly due to the lower size and lower polydispersity of N7, compared to N1 and N4 (Table S4). During lipolysis, all SNEDDS dispersions displayed the formation of similar colloidal structures, with minor differences. Bragg peaks started to appear after 10 min of lipolysis for N1 and N7 SNEDDS and after 15 min for N4 SNEDDS. The scattering vector for the single Bragg peaks were $q = 0.2$ $Å^{-1}$ for N1, N4 and N7 corresponding to a spacing of approximately 27.2 Å. This spacing corresponds to vesicular lamellar structures with bilayer spacing, and within the range of 25 to 40 Å [27].

When comparing the peak shapes, N1 and N4 (containing higher fractions of MCT and MGDG than N7) produced sharper peaks than N7 SNEDDS. Such differences may arise as the droplet size of N7 is smaller than for N1 and N4, leading to an imperfect lamellar structure, but still possessing a ratio integer corresponding to lamellar structures. The Bragg peak (Fig. 6d) of N1 and N4 SNEDDS had a higher AUC than N7, possibly due to a higher fraction of the digestible excipient MCT and MGDG, resulting in generation of more fatty acids and monoglycerides, forming the colloidal structures.

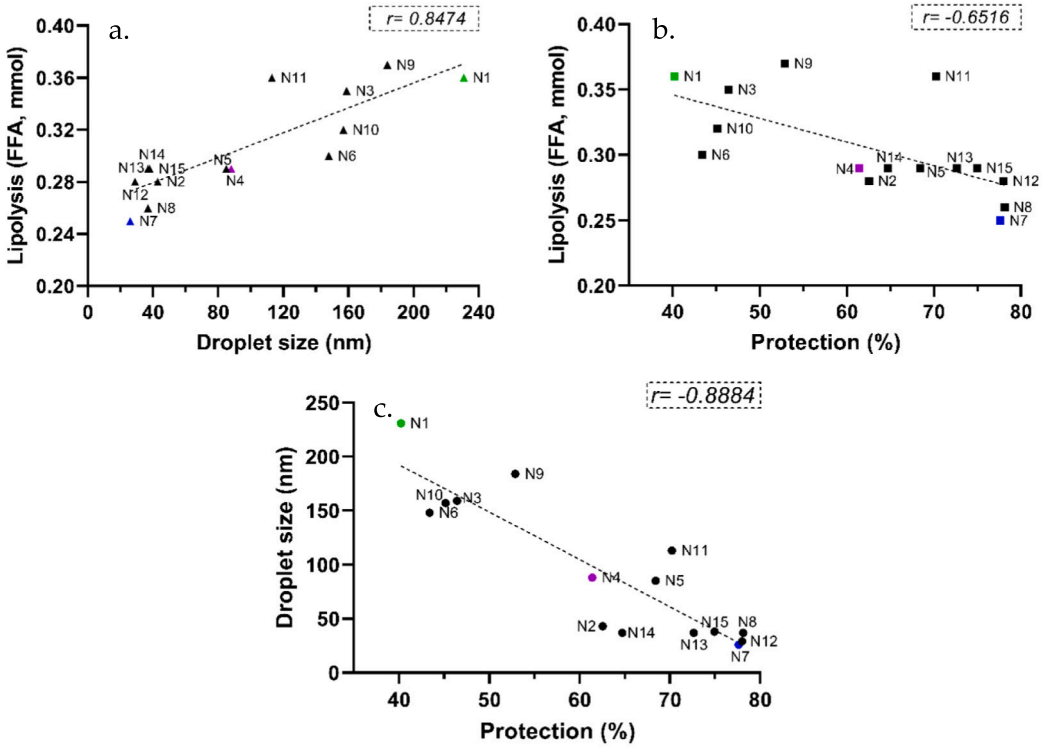

Fig. 5. Linear correlations between **a.** lipolysis (FFA; mmol) *vs* size (nm), **b.** Lipolysis (FFA; mmol) *vs* protection (%), **c.** Size (nm) *vs* protection (%). The points in each respective graph represent the observed value for each of the responses and r represents the Pearson's correlation coefficient.

Table 2
Droplet sizes (nm), lipolysis extent (FFA generated after 60 min) and % protected Ex (after 60 min of proteolysis) of the SNEDDS that were carried forward to *in situ* SAXS studies, *in vitro* cell permeability studies and *in vivo* pharmacokinetic studies. 10 % *w*/w MAPC is present in N1, N4 and N7 SNEDDS. All data are expressed as mean ± SD, $n = 3$.

Formulations	Lipid Excipients (wt%)			Responses		
	MCT	MGDG	Kolliphor®RH40	Size (nm)	FFA generated (mmol)	% Protected Ex
MCT rich (N1)	60	10	20	231 ± 8	0.36 ± 0.04	40.2 ± 1.5
MGDG rich (N4)	35	45	10	88 ± 7	0.29 ± 0.01	64.5 ± 5.5
Kolliphor®RH40 rich (N7)	30	30	30	26 ± 4	0.25 ± 0.01	77.6 ± 2.8

Based on the resemblance observed in the data, it is reasonable to infer that formulations N1, N4, and N7 share comparable characteristics during lipid digestion. All three SNEDDS exhibited the formation of lamellar structures during *in vitro* lipolysis, with only minor differentiating factors.

4.4. *In vitro permeability studies of the selected SNEDDS*

Fig. 7 (a and b) represents the TEER%, before and after incubation with N1, N4 and N7 SNEDDS, and the apparent permeability coefficient (P_{app}) of FD4 across the cell monolayers. Upon incubation of SNEDDS (along with FD4) with Caco-2 cells, there was a significant decrease *($p < 0.0001$)* in TEER% at 120 min for N4 and N7 SNEDDS, compared to N1 and the control (MES buffer). In addition, N4 and N7 SNEDDS resulted in a significantly higher P_{app} of FD4 ($p = 0.0063$ and *0.0047,* respectively) compared to N1 and the control. Even though N4 contains more MGDG than N7, there was no statistically significant differences in TEER% or P_{app} of FD4 between N4 and N7, indicating that above a certain MGDG level, there are not further permeability enhancing properties of SNEDDS.

MGDG and MAPC are known permeation enhancers, which can enable transport of macromolecules either *via* transcellular [28] or paracellular routes [29–31]. Accordingly, N4 and N7 SNEDDS containing higher fractions of MGDG and lower fractions of MCT, compared to N1, display a lower TEER and a higher FD4 P_{app}. This is also in agreement with Keemink et al. who found an increase in mannitol P_{app} across Caco-2 cell monolayer in the presence of SNEDDS with higher amounts of MGDG (≥ 30 % *w*/w) and lower amounts of MCT [31]. Kolliphor®RH40 is a non-ionic surfactant, which plays no or only a limited role in permeation enhancement [8]. Based on the results, it can be inferred that the selection of SNEDDS formulations with higher fractions of MGDG and lower fractions of MCT (*e.g.*, N4 and N7 SNEDDS) may have a positive impact on facilitating the transport of macromolecules, including peptides, across cell monolayers.

There was no discernible correlation observed between the *in situ* SAXS data coupled with *in vitro* lipolysis and the outcomes obtained from other *in vitro* techniques to evaluate SNEDDS (droplet size analysis, lipid digestion assessment, proteolytic protection of Ex, and Caco-2 cell permeability studies).

Overall, on assessing the *in vitro* properties of the SNEDDS in the given design space, SNEDDS with larger droplet size and extensive lipolysis (*e.g.*, N1) showed reduced protection of exenatide against proteolysis and lower permeation rates (P_{app}) for FD4 in Caco-2 studies. In contrast, SNEDDS with smaller droplet sizes and less lipolysis, displayed improved protection against proteolysis and also higher P_{app} values. The latter were characterized by having higher MGDG and

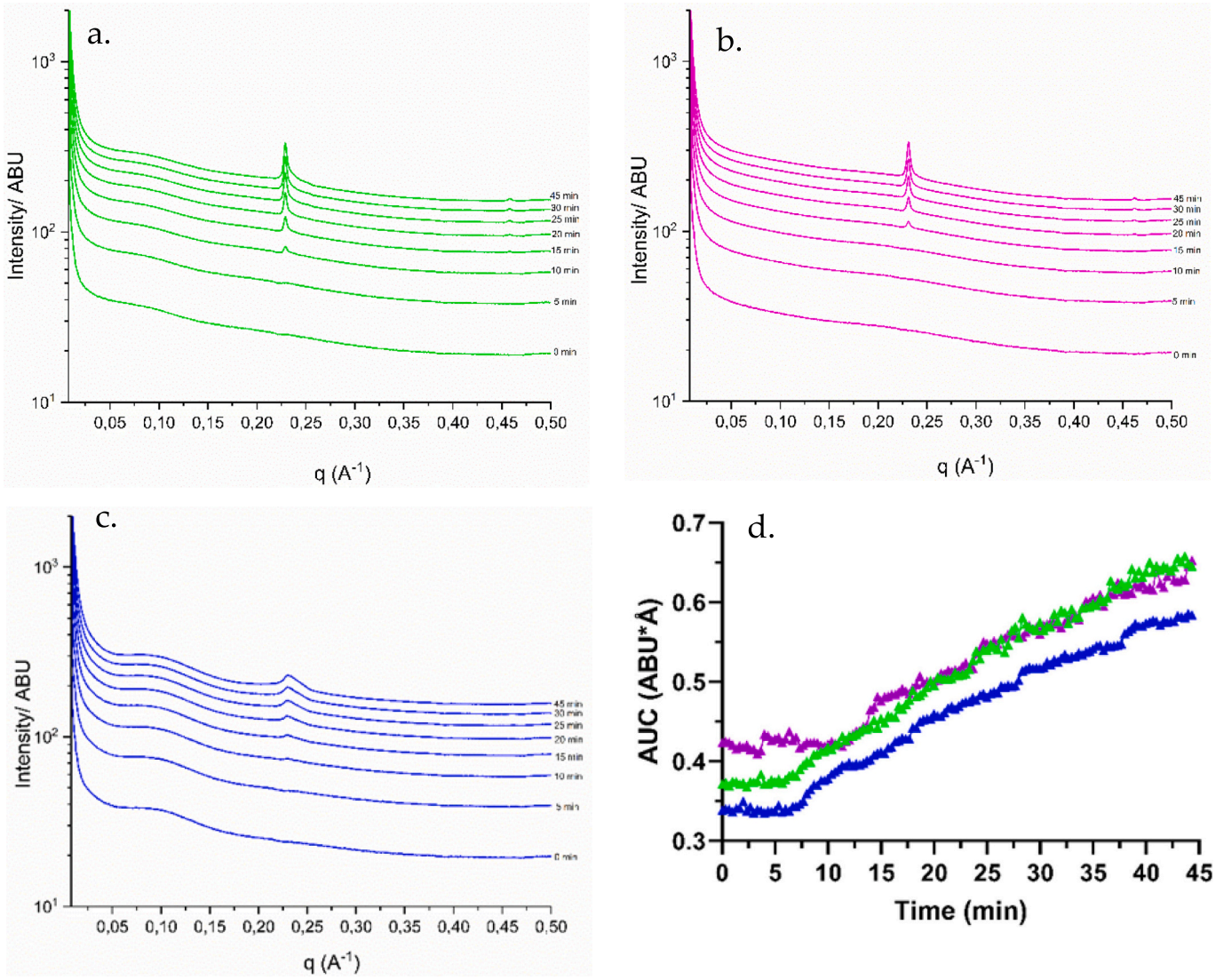

Fig. 6. *In situ* SAXS profiles (as single time points) during 45 min of *in vitro* lipolysis of **a.** N1- SNEDDS; **b.** N4- SNEDDS; **c.** N7-SNEDDS; **d.** Area under the curve of lamellar peaks (at q = 0.2 $Å^{-1}$) generated during 45 min lipolysis of N1- SNEDDS (green), N4- SNEDDS (purple) and N7-SNEDDS (blue). (For interpretation of the references to colour in this figure legend, the reader is referred to the web version of this article.)

Kolliphor®RH40 content (*e.g.*, N4 and N7), compared to N1 (Table 2 and Table S4).

4.5. Pharmacokinetic study in rats

Fig. 8 shows the mean plasma concentration-time profiles of Ex in the PK-Study. The maximum plasma concentration (C_{max}), time to reach C_{max} (T_{max}), bioavailability ($AUC_{0\text{-}8h}$), and relative bioavailability (%) are provided in Table 4.

The *s.c.* dosing of Ex represents 100 % $AUC_{0\text{-}8h}$, and resulted in significantly higher C_{max}, a faster T_{max} (except T_{max} for N1 ($p = 0.1476$)) and larger $AUC_{0\text{-}8h}$ when compared to the orally dosed of Ex:SPC-SNEDDS (Table 3). The oral dosing of Ex as a solution resulted in significantly lower C_{max}, a larger $AUC_{0\text{-}8h}$ (almost 5 to 10 fold lower), while no significant difference was observed for T_{max} when compared to the orally dosed of Ex:SPC-SNEDDS (Table 3). This exemplifies the challenges associated with oral administration of peptides, *i.e.* a bioavailability of ≤1 % [32,33].

Within the orally dosed groups, C_{max} of N7 SNEDDS was significantly higher ($p < 0.0001$), compared to both N1 and N4, while there were no significant differences for T_{max} of Ex between any of the SNEDDS ($p = 0.2449$). Both N4 and N7 SNEDDS resulted in statistically higher $AUC_{0\text{-}8h}$ than N1 SNEDDS ($p = 0.0399$ and $p = 0.0022$ respectively), however, there was no statistical difference between $AUC_{0\text{-}8h}$ of N7 and N4 SNEDDS ($p = 0.3408$).

The relative bioavailability observed in this study is lower than previously reported values, such as the 7 % relative bioavailability achieved with insulin:SPC loaded SNEDDS [10]. Additionally, Menzel et al. found a relative bioavailability of nearly 15 % with exenatide complexed with docusate in SNEDDS [34], highlighting the role of the complexing agent in order to improve the bioavailability of model peptide on oral administration.

Table 4 summarizes the correlations between the *in vitro* characteristics of selected SNEDDS and Ex:SPC-SNEDDS and their corresponding C_{max} and $AUC_{0\text{-}8h}$ values. The data suggests that droplet size and lipid digestion correlate negatively with C_{max} and $AUC_{0\text{-}8h}$, while proteolytic protection and P_{app} of FD4 correlate positively with these pharmacokinetic parameters. Thus, SNEDDS forming smaller droplets and with lower lipid digestion, such as for the SNEDDS with higher MGDG and Kolliphor®RH40 content, may protect the drug better and maintain its stability against protease upon exposure to the gastrointestinal environment. This enhanced stability could potentially prolong the retention

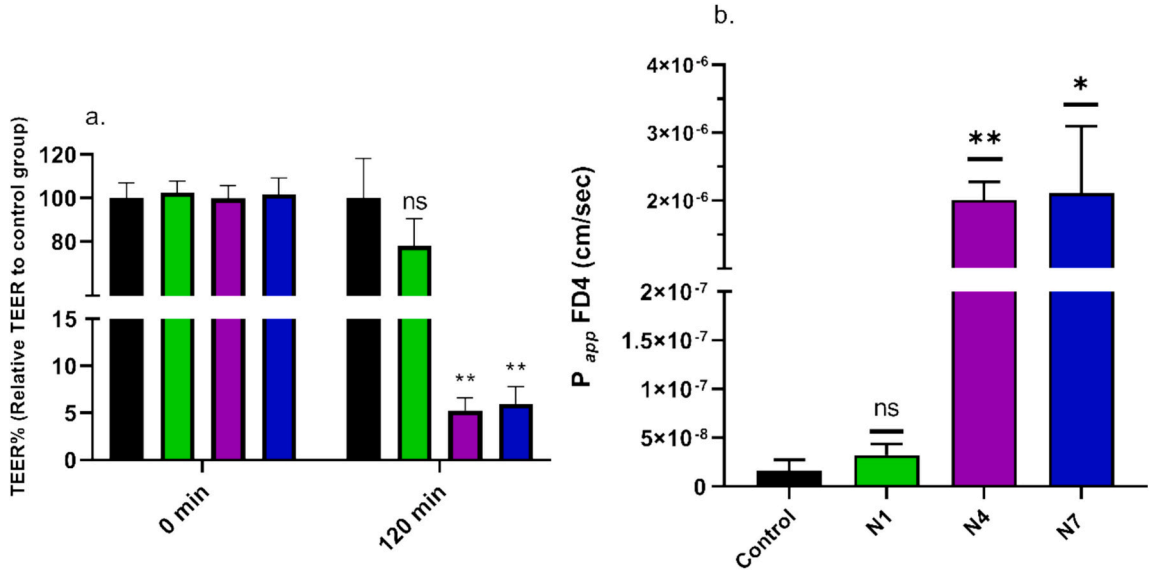

Fig. 7. **a.** Relative transepithelial electrical resistance (TEER%) values of Caco-2 cell monolayers before (0 min) and after (120 min) incubation at 37 °C with MES buffer (control; black), N1- SNEDDS (green), N4- SNEDDS (purple), and N7- SNEDDS (blue) dispersion (1:100 *v*/v); **b.** Apparent permeability coefficient (P_{app}) of FD4 across Caco-2 cell monolayer in the presence of MES buffer (control; black), N1- SNEDDS (green), N4- SNEDDS (purple), and N7- SNEDDS (blue) across Caco-2 cell monolayers. All results are expressed as mean ± SD ($n = 3$); *$p < 0.05$; **$p < 0.01$; ns: non-significant between control and N1 SNEDDS). (For interpretation of the references to colour in this figure legend, the reader is referred to the web version of this article.)

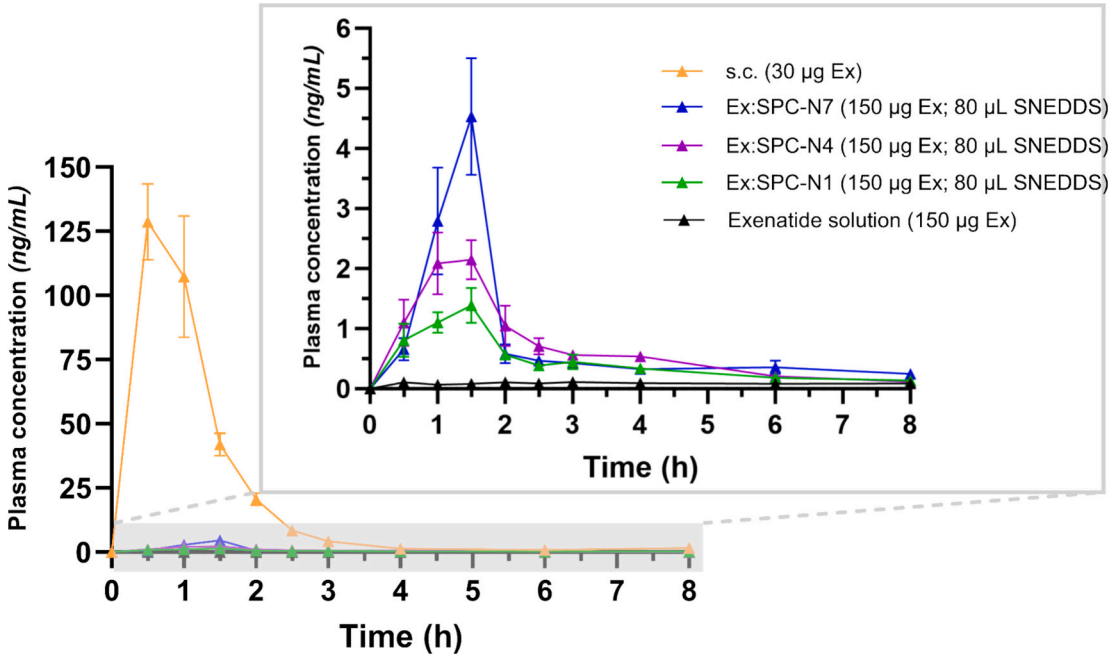

Fig. 8. Plasma concentration (ng/mL)-time (hours) profiles of Ex after oral administration of 150 µg Ex as Ex solution (black), as Ex:SPC loaded into N1-SNEDDS (green), N4-SNEDDS (purple) and N7-SNEDDS (blue) as 80 µL SNEDDS preconcentrate. Subcutaneously administered (yellow) Ex (30 µg) was used as positive control. All the results are expressed as mean ± SEM; $n = 6$. (For interpretation of the references to colour in this figure legend, the reader is referred to the web version of this article.)

of Ex within the lipid droplets, improving absorption. In contrast, SNEDDS forming larger droplets and being subjected to higher lipid digestion may result in more rapid breakdown, reducing the protective effect against proteases for the loaded peptide.

Overall, the data highlights the need to carefully balance droplet size, lipid digestion efficiency, and peptide protection to optimize SNEDDS formulations for oral peptide delivery. In the given design space, achieving this balance involved minimizing droplet size for better absorption, reducing the amount of FFA released during lipolysis, maintaining higher Ex stability against degradation and improving permeability across the cell monolayer. This approach, using a range of *in vitro* tools, can effectively guide the development of SNEDDS with enhanced oral bioavailability.

5. Conclusion

The objective of the study was to evaluate the efficacy of the *in vitro* methods specifically applied to the DoE-designed Ex:SPC complex-

Table 3
Pharmacokinetic (PK) parameters after oral or subcutaneous administration of Ex to fasted rats. Data presented as mean ± SEM (n = 6).

Formulations	C_{max} (ng/mL)	T_{max} (h)	$AUC_{0\text{-}8h}$ (ng*h/mL)	Relative bioavailability (%)
s.c.	142.9 ± 14.3	0.7 ± 0.1	161.9 ± 19.7	100
Ex solution	0.1 ± 0.0	2.1 ± 0.9	0.7 ± 0.1	–
N1	1.8 ± 0.2[a]	1.1 ± 0.2	3.5 ± 0.3[d]	0.4 ± 0.0[f]
N4	2.8 ± 0.3[b]	1.4 ± 0.1	5.3 ± 0.6[e]	0.7 ± 0.1[g]
N7	5.8 ± 0.4[c]	1.3 ± 0.3	6.3 ± 0.4[e]	0.8 ± 0.1[g]

Values with "a" are significantly different from values with "b" and "c" ($p < 0.05$). Values with "b" are significantly different from values with "c" ($p < 0.05$). Values with "d" are significantly different from values with "e" ($p < 0.05$). Values with "f" are significantly different from values with "g" ($p < 0.05$).

Table 4
Summary table of correlations between the *in vitro* evaluations of the three selected SNEDDS and the PK-parameters. The green, purple and blue represent N1-, N4- and N7-SNEDDS.

	C_{max} (ng/mL)	$AUC_{0\text{-}8h}$ (ng*h/mL)
Droplet size (nm)	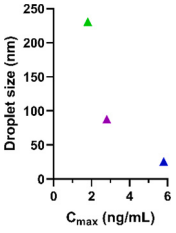	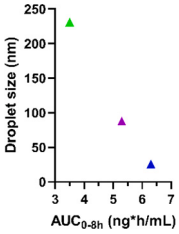
Lipolysis (FFA; mmol)	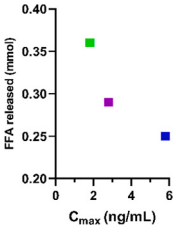	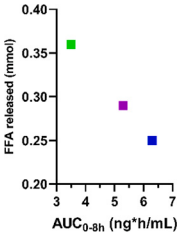
Proteolysis (%Exenatide protected)	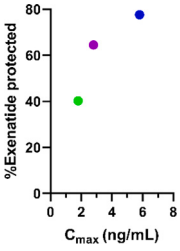	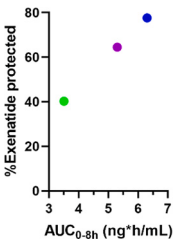
Caco-2 cell permeability (P_{app}; cm/s)	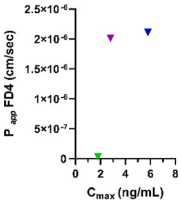	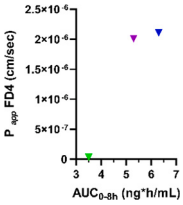

containing SNEDDS, in predicting the absorption of Ex following oral gavage in rats. SNEDDS compositions with higher MGDG and Kolliphor® RH40 (N4 and N7 SNEDDS) displayed smaller droplet sizes, lower extent of *in vitro* lipolysis, better proteolytic protection, and higher permeation across Caco-2 monolayers, leading to improved Ex absorption after oral administration. In contrast, N1 SNEDDS with higher MCT exhibited larger droplet sizes, increased lipolysis, reduced proteolytic protection, and lower Caco-2 permeation, resulting in reduced Ex absorption upon oral administration. These findings provide insights into *in vitro* approaches that can be adopted to understand formulation characteristics that impact Ex absorption, guiding design strategies for improved oral absorption of peptides.

Funding

The research was financially supported by the Phospholipid Research Center, Heidelberg, Germany (AMU-2019-071/2-1) and the Brødrene Hartmanns Fond, Copenhagen, Denmark (A37218).

CRediT authorship contribution statement

Ramakrishnan Venkatasubramanian: Writing – original draft, Methodology, Investigation, Conceptualization. **Passant M. Al-Maghrabi:** Writing – review & editing, Methodology, Investigation. **Oscar Alavi:** Writing – review & editing, Methodology, Investigation. **Tania Lind:** Writing – review & editing, Supervision, Methodology. **Philip Jonas Sassene:** Writing – review & editing, Methodology. **Jacob J.K. Kirkensgaard:** Writing – review & editing, Methodology. **Pablo Mota-Santiago:** Writing – review & editing, Methodology. **Thomas Rades:** Writing – review & editing, Supervision, Methodology, Conceptualization. **Anette Müllertz:** Writing – review & editing, Supervision, Resources, Project administration, Methodology, Funding acquisition, Conceptualization.

Declaration of competing interest

The authors declare that they have no competing financial interests or personal relationships that could have appeared to influence the work in this manuscript.

Declaration of generative AI in scientific writing.

During the preparation of this work, the author(s) used ChatGPT, an AI language model developed by OpenAI, in order to improve grammar, readability, and language. After using this tool, the author(s) reviewed and edited the content as needed and take(s) full responsibility for the content of the publication.

Acknowledgements

Mette Frandsen and Heidi Fosgerau are acknowledged for their assistance with cell culturing. We acknowledge Bachem for supplying exenatide for the purpose of this project. We acknowledge the MAX IV Laboratory for time on the CoSAXS beamline under Proposal 20210947. Research conducted at MAX IV, a Swedish national user facility, is supported by the Swedish Research Council under contract 2018-07152, the Swedish Governmental Agency for Innovation Systems under contract 2018-04969, and Formas under contract 2019-02496. Jacob R. Jørgensen is acknowledged for his support in conducting the *in vivo* studies. The graphical abstract was created using Biorender.com.

Appendix A. Supplementary data

Supplementary data to this article can be found online at https://doi.org/10.1016/j.jconrel.2025.01.013.

Data availability

Data will be made available on request.

References

[1] S. Haddadzadegan, F. Dorkoosh, A. Bernkop-Schnürch, Oral delivery of therapeutic peptides and proteins: technology landscape of lipid-based nanocarriers, Adv. Drug Deliv. Rev. 182 (2022).

[2] P. Li, H.M. Nielsen, A. Müllertz, Oral delivery of peptides and proteins using lipid-based drug delivery systems, Expert Opin. Drug Deliv. 9 (2012) 1289–1304.

[3] P. Li, H.M. Nielsen, M. Fano, A. Müllertz, Preparation and characterization of insulin-surfactant complexes for loading into lipid-based drug delivery systems, J. Pharm. Sci. 102 (2013) 2689–2698.

[4] P. Li, A. Tan, C.A. Prestidge, H.M. Nielsen, A. Müllertz, Self-nanoemulsifying drug delivery systems for oral insulin delivery: in vitro and in vivo evaluations of enteric coating and drug loading, Int. J. Pharm. 477 (2014) 390–398.

[5] K.D. Ristroph, Prud'homme, R. K., Hydrophobic ion pairing: encapsulating small molecules, peptides, and proteins into nanocarriers, Nanoscale Adv. 1 (2019) 4207–4237.

[6] C. Dumont, S. Bourgeois, H. Fessi, V. Jannin, Lipid-based nanosuspensions for oral delivery of peptides, a critical review, Int. J. Pharm. 541 (2018) 117–135.

[7] S. Maher, R.J. Mrsny, D.J. Brayden, Intestinal permeation enhancers for oral peptide delivery, Adv. Drug Deliv. Rev. 106 (2016) 277–319.

[8] S. Maher, C. Geoghegan, D.J. Brayden, Intestinal permeation enhancers to improve oral bioavailability of macromolecules: reasons for low efficacy in humans, Expert Opin. Drug Deliv. 18 (2021) 273–300.

[9] D.J. Brayden, Evolving peptides for oral intake, Nat. Biomed. Eng. 4 (2020) 487–488.

[10] Q. Zhang, et al., The in vitro and in vivo study on self-nanoemulsifying drug delivery system (SNEDDS) based on insulin-phospholipid complex, J. Biomed. Nanotechnol. 8 (2012) 90–97.

[11] J. Liu, et al., SEDDS for intestinal absorption of insulin: application of Caco-2 and Caco-2/HT29 co-culture monolayers and intra-jejunal instillation in rats, Int. J. Pharm. 560 (2019) 377–384.

[12] D.J. Brayden, T.A. Hill, D.P. Fairlie, S. Maher, R.J. Mrsny, Systemic delivery of peptides by the oral route: formulation and medicinal chemistry approaches, Adv. Drug Deliv. Rev. 157 (2020) 2–36.

[13] T. Karamanidou, et al., Effective incorporation of insulin in mucus permeating self-nanoemulsifying drug delivery systems, Eur. J. Pharm. Biopharm. 97 (2015) 223–229.

[14] J. Liu, C. Hirschberg, M. Fanø, H. Mu, A. Müllertz, Evaluation of self-emulsifying drug delivery systems for oral insulin delivery using an in vitro model simulating the intestinal proteolysis, Eur. J. Pharm. Sci. 147 (2020) 105272.

[15] S.Y.K. Fong, A. Ibisogly, A. Bauer-Brandl, Solubility enhancement of BCS class II drug by solid phospholipid dispersions: spray drying versus freeze-drying, Int. J. Pharm. 496 (2015) 382–391.

[16] N.H. Zangenberg, A. Müllertz, H.G. Kristensen, L. Hovgaard, A dynamic in vitro lipolysis model I. Controlling the rate of lipolysis by continuous addition of calcium, Eur. J. Pharm. Sci. 14 (2001) 115–122.

[17] P. Ågren, et al., Kinetics of Cosurfactant-surfactant-silicate phase behavior. 1. Short-chain alcohols, J. Phys. Chem. B 103 (1999) 5943–5948.

[18] C. Zhou, X. Xia, Y. Liu, L. Li, The preparation of a complex of insulin-phospholipids and their interaction mechanism, J. Pept. Sci. 18 (2012) 541–548.

[19] J. Engsbli, W.A. Kleinmans, L. Singhll, G. Singhi, J.-P. Raufmanll, Isolation and characterization of exendin-4, an exendin-3 analogue, from *Heloderma suspectum* venom. Further evidence for an exendin receptor on dispersed acini from guinea pig pancreas, J. Biol. Chem. 267 (1992) 7402–7406.

[20] S.N. Politis, P. Colombo, G. Colombo, D.M. Rekkas, Design of experiments (DoE) in pharmaceutical development, Drug Dev. Ind. Pharm. 43 (2017) 889–901.

[21] A. Christiansen, T. Backensfeld, W. Weitschies, Effects of non-ionic surfactants on in vitro triglyceride digestion and their susceptibility to digestion by pancreatic enzymes, Eur. J. Pharm. Sci. 41 (2010) 376–382.

[22] G. Leonaviciute, O. Zupančič, F. Prüfert, J. Rohrer, A. Bernkop-Schnürch, Impact of lipases on the protective effect of SEDDS for incorporated peptide drugs towards intestinal peptidases, Int. J. Pharm. 508 (2016) 102–108.

[23] R. Mahjub, F.A. Dorkoosh, M. Rafiee-Tehrani, A. Bernkop Schnürch, Oral self-nanoemulsifying peptide drug delivery systems: impact of lipase on drug release, J. Microencapsul. 32 (2015) 401–407.

[24] G. Hetényi, et al., Comparison of the protective effect of self-emulsifying peptide drug delivery systems towards intestinal proteases and glutathione, Int. J. Pharm. 523 (2017) 357–365.

[25] S. Battista, et al., UV Properties and Loading into Liposomes of Quinoline Derivatives, 2021.

[26] R. Takahashi, T. Narayanan, S.I. Yusa, T. Sato, Formation kinetics of polymer vesicles from spherical and cylindrical micelles bearing the polyelectrolyte complex core studied by time-resolved USAXS and SAXS, Macromolecules 55 (2022) 684–695.

[27] D. Marsh, Handbook of Lipid Bilayers, Taylor & Francis Group, 2013.

[28] A. Bernkop-Schnürch, Low molecular mass permeation enhancers in oral delivery of macromolecular drugs, in: Oral Delivery of Macromolecular Drugs, Springer, 2009, pp. 85–101.

[29] J.C. Kim, E.J. Park, D.H. Na, Gastrointestinal permeation enhancers for the development of oral peptide pharmaceuticals, Pharmaceuticals 15 (2022) 1585.

[30] T. Lindmark, T. Nikkilä, P. Artursson, Mechanisms of absorption enhancement by medium chain fatty acids in intestinal epithelial Caco-2 cell monolayers, J. Pharmacol. Exp. Ther. 275 (1995) 958.

[31] J. Keemink, C.A.S. Bergström, Caco-2 cell conditions enabling studies of drug absorption from digestible lipid-based formulations, Pharm. Res. 35 (2018).

[32] Y. Sun, et al., An investigation into the gastrointestinal stability of exenatide in the presence of pure enzymes, everted intestinal rings and intestinal homogenates, Biol. Pharm. Bull. 39 (2016).

[33] M. Celik-Tekeli, N. Celebi, M.Y. Tekeli, Y. Aktas, Evaluation of the hypoglycemic effect of exendin-4's new oral self-nanoemulsifying system in rats, Eur. J. Pharm. Sci. 158 (2021).

[34] C. Menzel, et al., In vivo evaluation of an oral self-emulsifying drug delivery system (SEDDS) for exenatide, J. Control. Release 277 (2018) 165–172.